Sigma Journal of Engineering and Natural Sciences
Web page info: https://sigma.yildiz.edu.tr
DOI: 10.14744/sigma.2026.2034

Research Article

Numerical simulation of magnetohydrodynamic casson Williamson hybrid nanofluid flow accounting thermal stratification

Jintu Mani NATH[1,2,*], Ashish PAUL[2], Tusar Kanti DAS[2,3]

[1]*Department of Mathematics, Mangaldai College (Autonomous), Mangaldai, 784125, India*
[2]*Department of Mathematics, Cotton University, Guwahati, 781001, India*
[3]*Department of Mathematics, Dudhnoi College (Autonomous), Dudhnoi, 783124, India*

ARTICLE INFO

Article history
Received: 13 June 2024
Revised: 21 August 2024
Accepted: 11 November 2024

Keywords:
Heat Stratification; Hybrid Nanofluid; Vertically Stretching Cylinder; Volume Concentration; Williamson Fluid

ABSTRACT

This study investigates the thermally stratified magnetohydrodynamic flow of Casson-Williamson hybrid nano liquid around a linearly stretched vertical cylinder in a porous region. The unique aspect of this research is the inclusion of thermal stratification effects on non-Newtonian hybrid nanofluid flow. Computational solutions are derived by employing MATLAB's Bvp4c algorithm, with velocity and thermal profiles illustrated graphically, and distinct non-dimensional factors. Shear and thermal transmission rates are also calculated and displayed in tables. Results expose that thermal stratification reduces the thermal profile, with notable heat stratification, even causing negative temperature values. It's also shown that the Williamson hybrid nanofluid exhibits a 16.5% increase in heat transmission rate over the Williamson nanofluid and a 30.7% higher shear stress rate. The heat transmission rate is enhanced by increasing the thermal buoyancy factor but decreases with higher values of the Casson factor, thermal stratification factor, porosity factor, and Weissenberg number. Additionally, the thermal distribution increases with a higher Weissenberg number and curvature factor. These findings offer substantial potential for enhancing thermal management in various industrial applications, marking a significant contribution to fluid mechanics and nanofluid research. The outcomes align well with prior studies.

Cite this article as: Nath JM, Paul A, Das TK. Numerical simulation of magnetohydrodynamic casson Williamson hybrid nanofluid flow accounting thermal stratification. Sigma J Eng Nat Sci 2026;44(2):1240–1250.

INTRODUCTION

Nanofluids are engineered fluids containing nanoparticles that augment thermal conductivity and thermal transmission. They are broadly operated in solar energy applications, thermal exchangers, and electronics cooling structures. Nanofluids boost thermal performance, which increases the efficacy of heating and cooling systems in a variety of industries, such as energy production, automotive, and aerospace. Kataria and Mittal [1] investigated the velocity and temperature of gravity-based convective nanofluid

***Corresponding author.**
*E-mail address: nathjintu67@gmail.com

This paper was recommended for publication in revised form by Editor-in-Chief Ahmet Selim Dalkilic

movement via a vertical plate in the existence of a magnetic field. Moreover, Sheikholeslami et al. [2] explored the radiation influences on thermal transmission of nanofluid flow incorporating heat interfacial resistance. Furthermore, many researchers [3-9] explored distinct nanofluid flow phenomena incorporating various conditions. Moreover, a new sort of fluid that can offer noteworthy heat transport for a diverse range of industrial sectors is essential due to the significance of the improvement of nanotechnology. Thus, a unique fluid known as a hybrid nanofluid was created. The recent discovery of hybrid nanofluid has prompted multiple researchers to expand their numerical and experimental work. A hybrid nano-liquid may be formed by scattering several sorts of nano-particles in one or more fundamental fluids. In comparison to conventional nanofluids, hybrid nanofluids exhibit more thermal traits. These fluids are used in freezing, thermoelectric refrigeration, electronic cooling processes, medical applications, and more.

The heat transportation augmentation in hydro-magnetic Al_2O_3 - Cu hybrid nano-liquid movement via an extending cylinder was designated by Maskeen et al. [10]. Their findings indicate that related to conventional fluids or nanofluids, hybrid nanofluids are more effective at transmission of heat. Additionally, Khashi'ie et al. [11] used a porous longitudinal cylinder to track the flow of a hybrid nanofluid near its stagnation point, showing an effect on temperature stratification. Throughout their examination in a contracting cylinder, Al_2O_3-water nanofluid performed at a lower heat transfer rate than Cu-Al_2O_3/water hybrid nanofluids. Additionally, Elsaid et al. [12] conducted a computational study on the impact of a hybrid nanofluid's performance across a rotating cylinder. Also, Khan et al. [13] investigated the radiative movement created by the hybrid nano-liquid in a porous vertical cylinder. Recently, Nath et al. [14] performed computational comparative research on magnetohydrodynamics stagnation point movement of hybrid nanofluids flow with different fundamental fluids.

The utmost stimulating area of investigation is the inquiry of fluid movement via stretched cylinders. Applications for flow throughout a stretching cylinder encompass wire drawing, fiber spinning, and polymer extrusion operations, where regular stretching advances material features. In refrigeration systems, chemical reactors, and filtering units, it is vital to optimize heat and mass transmission. Furthermore, controlled stretching impacts thermal conductivity and viscosity, and also enhances system efficiency. In these scenarios, this is crucial for the development of biomedical devices and thermal exchangers. Crane [15] first studied how a stretched cylinder caused the boundary layers to flow. Wang [16] then investigated the flow of a viscous fluid across a stretched, hollow cylinder. Waqas et al. [17] recently used a vertically elongating cylinder to study the process of thermal conduction in a magnetised motion of hybrid nanoliquids. Additionally, to ascertain the procedure of thermal transmission integrating the movement of hybrid nanofluids via an extended cylinder, Sreenivasa et al. [18] conducted numerical research. Recently, Nath et al. [19] investigated the Newtonian and non-Newtonian hybrid nanofluid movement in cylindrical geometry.

The flow and thermal transmission features of non-Newtonian fluids are noteworthy to diverse systems in bioengineering and pharmacological medicine. Therefore, despite its intricacy, applied mathematician's quintessence on it. Hamid et al. [20] investigated the effect of thermal radiation on Williamson nanofluid movement. After that, the study of Khan et al. [21] emphasized how heat stratification influence with the viscosity of Williamson nano-liquid movement. Also, Mittal et al. [22] investigated the combined convection micropolar ferrofluid movement incorporating viscous dissipation, joule heating, and convective boundary limitations. Furthermore, Mittal and Patel [23] examined the consequences of thermophoresis and Brownian motion on combined convection MHD Casson fluid movement. Also, Nath et al. [24] addressed the thermal transport features of magnetohydrodynamic stratified Casson hybrid nanofluid movement via a porous extending cylinder. Additionally, Hussain et al. [25] considered the Williamson fluid with homogeneous-heterogeneous interactions in an assessment of sheet and cylinder on MHD convective flow. The results demonstrate that fluid flow and concentration are more noticeable by cylinder than by sheet. Williamson nanofluid movement in a convective cylinder with heat radiation and variable conductivity was investigated by Bilal et al. [26]. A. Almaneea [27] quantitatively studied the enhancement of heat and mass transfer in MHD Williamson fluid using hybrid nanoparticles. Recently a few researchers [28-33] have investigated in the field of non-Newtonian fluid incorporating distinct conditions.

Researchers have thoroughly investigated the role that thermal and solute stratification plays in the transmission of heat and mass. Stratification in flow domains may result from variations in fluid temperature, density, or concentration. Salinity, seismic fluxes, lake thermo-hydraulics, and underground water supplies are all affected by the process of heat stratification. Srinivasacharya and Surender [34-37] examined the stratified nanofluid movement via a vertical plate. Also, Srinivasacharya et al. [38] computationally studied the doubly stratified free convection in a non-darcy porous medium. Through the Keller box approach, Bilal et al. [39] numerically computed the thermally stratiform Williamson liquid movement. The findings illustrate that the thermal transmission rate exhibits prominent development for ascending magnitudes of Prandtl number for cylindrical geometry relatively for plane geometry. Williamson nanofluid flow's variation in viscosity as a consequence of heat and solute stratification was addressed by Khan et al. [40]. Furthermore, radiative bi-nano-liquid movement on a curved outward under temperature stratification circumstances was investigated computationally by Ramzan et al. [41]. Khan et al. investigated the flow and heat transport of a bio-convective hybrid nanofluid that included triple stratification impacts [42]. Masood et al. investigated the effects

of radiation and heat stratification on a hybrid nanofluid [43]. Heat stratification and unequal thermal radiation in the hybrid nanofluid movement were studied by Manzoor et al. [44]. Kairi et al. [45] studied the layered thermo-solutal Marangoni bioconvective movement of gyrotactic microbes in Williamson nanofluid. Moreover, an array of investigations [46-54] explored into different flow phenomena observed in the conventional fluid or hybrid nanofluids over numerous constraints.

The vitality of the Cassion Williamson hybrid nanofluid flow through solid geometries is brought out by the literature assessment, which additionally stimulates further research in this discipline. Casson Williamson hybrid nanofluid flow problems over vertical cylindrical bodies are also infrequently discussed in the literature. Nobody has inspected the flow of Casson Williamson hybrid nanofluid integrating the thermal stratification impact over a linearly stretched vertical cylinder. Which provides the required novelty for the current investigation. So, motivated by this, the present exploration investigates how heat stratification influences the MHD Casson Williamson Ethylene glycol driven MoS_2 - *Cu* hybrid nano-liquid movement via a stretched vertical cylinder in a permeable region incorporating the utilization of an inclined magnetic field. In this study integrating *Cu* and MoS_2 nanoparticles augment the lubricating, thermal transmission, and heat conductivity of nanofluids. MoS_2 has superior lubrication, stability, and anti-friction features, whereas *Cu* nanoparticles have prodigious heat conductivity, improving cooling efficiency. Also choosing Ethylene glycol offers a low-freezing, greater-boiling point base fluid. This amalgamation advances thermal transmission, diminishes friction, and escalates system stability, making it perfect for lubrication, cooling, and energy-efficient applications in the electronics and automotive industries. The fundamental objective of this investigation is to address the following queries:

- What are the outcomes and features of the flow under the specific conditions?
- What impact does the existence of MoS_2, and Cu nanoparticles influence the flow behavior and heat transport?
- How does the strong thermal stratification impact influence the Casson Williamson hybrid nanofluid?
- How does the Weissenberg number and curvature factor affect the thermal curve and the rate of thermal transmission?
- What insights can be gained from this investigation on the non-Newtonian hybrid nanofluid flow via a stretching cylinder?

Bvp4c [55] approach is employed to solve the non-linear ODE arrangement. Tabulated data are used to signify and compare several parameters visually. This study has an extensive range of applications. It is indispensable for maximizing thermal transmission in industrial operations, including energy storage, chemical and nuclear reactors, and cooling mechanisms. It also supports greater magnetic fluid-based technologies in engineering and medicine, improved oil recovery, heat insulation frameworks, and biomedical fluid dynamics.

Mathematical Formulation

We examine a stable Casson Williamson hybrid nanofluid that passes via a vertical cylinder that is stretched and linearly permeable. In this flow issue, the coordinate system used is cylindrical polar (x,r), where x and r indicate the axial and radial directions, correspondingly. Also, the magnetic field of strength B_0 is applied vertically at an angle of ξ. The momentum equation also incorporates the impact of heat buoyancy. The cylinder expands linearly, while integrating the surface velocity, $w_w = a\left(\frac{x}{l}\right)$, employing with its axis. In which a and l denote the velocity and characteristic-length of the cylinder. $T_w(x) = T_0 + E\left(\frac{x}{l}\right)$ is considered to be wall temperature and $T_\infty(x) = T_0 + F\left(\frac{x}{l}\right)$ is the surrounding

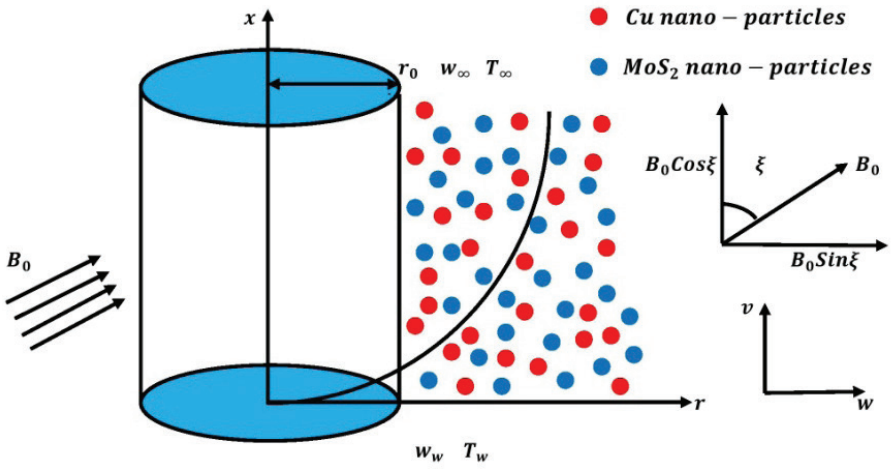

Figure 1. Representation of the flow model.

temperature; in which E, F and T_0 symbolize positive constants ($E > F$)and initial temperature, respectively.

Figure 1 represents the flow model of this study.

The governing equations are as follows (Ref. [27, 56-61]):

$$\frac{\partial(rw)}{\partial x} + \frac{\partial(rv)}{\partial r} = 0 \tag{1}$$

$$\begin{aligned} w\frac{\partial w}{\partial x} + v\frac{\partial w}{\partial r} &= (1+\tfrac{1}{B})\frac{\mu_{hnf}}{\rho_{hnf}}\frac{1}{r}\frac{\partial}{\partial r}\left(r\frac{\partial w}{\partial r}\right) \\ &- (1+\tfrac{1}{B})\frac{\mu_{hnf}}{\rho_{hnf}}\left(\sqrt{2}\Gamma\frac{\partial w}{\partial r}\frac{\partial^2 w}{\partial r^2} + \frac{\Gamma}{\sqrt{2}}\frac{1}{r}\left(\frac{\partial w}{\partial r}\right)^2\right) \\ &+ \frac{(\rho\beta)_{hnf}}{\rho_{hnf}}g(T-T_\infty) - \frac{\sigma_{hnf}}{\rho_{hnf}}{B_0}^2.Sin^2\xi.w \\ &- \frac{\mu_{hnf}}{\rho_{hnf}}\frac{w}{k}(1+\tfrac{1}{B}) \end{aligned} \tag{2}$$

$$w\frac{\partial T}{\partial x} + v\frac{\partial T}{\partial r} = \frac{k_{hnf}}{(\rho c_p)_{hnf}}\frac{1}{r}\frac{\partial}{\partial r}\left(r\frac{\partial T}{\partial r}\right) \tag{3}$$

The boundary constraints are:

$$\begin{aligned} &w = a\frac{x}{l},\ \ v = 0,\ \ \ T = T_w(x) \ \ \ while\ r = r_0 \\ &w = 0\ ,\ \ T \to T_\infty(x) \qquad\qquad\ \ while\ r \to \infty \end{aligned} \tag{4}$$

The similarity transformations [61] are as follows:

$$\eta = \frac{r^2 - {r_0}^2}{2r_0}\sqrt{\frac{a}{\upsilon_f l}},\ \psi = \sqrt{\frac{a\upsilon_f}{l}}xr_0 f(\eta),\ \theta = \frac{T-T_\infty(x)}{T_w(x)-T_0} \tag{5}$$

Where $w = \frac{1}{r}\frac{\partial\psi}{\partial r}$, $v = -\frac{1}{r}\frac{\partial\psi}{\partial x}$

The transformed dimensionless nonlinear equations, taking into account the previously indicated transformation, are described as follows:

$$\begin{aligned} f'^2 - f.f'' &= (1+\tfrac{1}{B})\left(\frac{\rho_f}{\rho_{hnf}}\frac{\mu_{hnf}}{\mu_f}\right)\{2\gamma f'' + (1+2\gamma\eta)f'''\} \\ &+ \left(\frac{\rho_f}{\rho_{hnf}}\frac{\mu_{hnf}}{\mu_f}\right)(1+\tfrac{1}{B})\{3.We.\gamma(1+2\gamma\eta)^{\frac{1}{2}}f''^2 \\ &+ 2We(1+2\gamma\eta)^{\frac{3}{2}}f''.f'''\} + (\frac{\rho_f}{\rho_{hnf}}\frac{(\rho\beta)_{hnf}}{(\rho\beta)_f})\,\lambda.\theta \\ &- \{Sin^2\xi.\left(\frac{\rho_f}{\rho_{hnf}}\frac{\sigma_{hnf}}{\sigma_f}\right)M + \left(\frac{\rho_f}{\rho_{hnf}}\frac{\mu_{hnf}}{\mu_f}\right)P(1+\tfrac{1}{B})\}f' \end{aligned} \tag{6}$$

$$\begin{aligned} f'(\theta+\delta) - f\theta' = \left(\frac{k_{hnf}}{k_f}\frac{(\rho c_p)_f}{(\rho c_p)_{hnf}}\right)\left(\frac{1}{Pr}\right)\{2\gamma\theta' \\ + (2\gamma\eta+1)\theta''\} \end{aligned} \tag{7}$$

The transformed boundary restrictions are represented as:

$$\begin{aligned} &f'(0) = 1,\ \ f(0) = 0 \\ &\theta(0) = 1-\delta,\ \ \ f'(\infty)\to 0,\ \ \ \theta(\infty)\to 0 \end{aligned} \tag{8}$$

In which,

$$M = \frac{{B_0}^2 l\sigma_f}{a\rho_f},\ P = \frac{l}{a}\frac{\vartheta_f}{k},\ \gamma = \sqrt{\frac{l\vartheta_f}{a{r_0}^2}},$$

$$\lambda = \frac{Gr_x}{{Re_x}^2},\ \delta = \frac{F}{E}\ , Pr = \frac{\vartheta_f(\rho c_p)_f}{k_f}, We = \frac{\Gamma a^{3/2}x}{\sqrt{2\nu}l^{3/2}}$$

The density ρ_{hnf}, thermal conductivity k_{hnf}, heat expansion $(\rho\beta)_{hnf}$, heat capacity $(\rho C_p)_{hnf}$, dynamic viscosity μ_{hnf} of hybrid nano-fluid is specified as follows (Ref. [56, 61]):

$$\rho_{hnf} = (1-\phi_2)\{(1-\phi_1)\rho_f + \phi_1\rho_{s1}\} + \phi_2\rho_{s2}\ ,$$

$$k_{hnf} = k_{bf}\left\{\frac{k_{s2}+2k_{bf}-2\phi_2(k_{bf}-k_{s2})}{k_{s2}+2k_{bf}+\phi_2(k_{bf}-k_{s2})}\right\}$$

$$\text{Where } k_{bf} = k_f\left\{\frac{k_{s1}+2k_f-2\phi_1(k_f-k_{s1})}{k_{s1}+2k_f+\phi_1(k_f-k_{s1)}}\right\},$$

$$(\rho\beta)_{hnf} = (1-\phi_2)\{(1-\phi_1)(\rho\beta)_f + \phi_1(\rho\beta)_{s1}\} + \phi_2(\rho\beta)_{s2}\ ,$$

$$\mu_{hnf} = \frac{\mu_f}{(1-\phi_1)^{2.5}(1-\phi_2)^{2.5}}\ ,$$

$$(\rho C_p)_{hnf} = (1-\phi_2)\left\{(1-\phi_1)\left(\rho C_p\right)_f + \phi_1\left(\rho C_p\right)_{s1}\right\} + \phi_2\left(\rho C_p\right)_{s2}$$

Moreover, , the skin friction and the thermal transport rate are indicated by:

$$C_f {Re_x}^{1/2} = \frac{1}{(1-\phi_1)^{2.5}(1-\phi_2)^{2.5}}(1+\tfrac{1}{B})\left(f''(0) + \frac{We}{2}f''(0)^2\right)$$

$$Nu_x {Re_x}^{-1/2} = -\frac{k_{hnf}}{k_f}\theta'(0)$$

METHODOLOGY

The dimensionless higher order ODEs (6)– (7) are transformed into first-order boundary value problem integrating with the associated boundary conditions (8). The formerly mentioned non-dimensional ODEs are numerically included using MATLAB's bvp4c method in conjunction with a shooting strategy. Even for complex and disordered formulations, the bvp4c solver produces correct results by more precisely addressing boundary value issues. Its powerful mesh augmentation mechanism reduces computational burden and increases computation efficiency. In the meantime, using the bvp4c solver requires a preliminary projection that satisfies its spatial constraints. With a convergence threshold of 10^{-6}, Bvp4c is by far the superlative method for computing the outcomes.

RESULTS AND DISCUSSION

The thermally stratified Casson Williamson Ethylene glycol driven MoS_2 - Cu hybrid nanofluid movement via a stretched vertical cylinder is investigated in this research. To produce a hybrid nanofluid, molybdenum disulfide

Table 1. Thermo physical appearances of base fluid and nano particles [56,60] [created by author]

Thermo-physical attributes	$\rho(kg/m^3)$	$C_p(J/kgK)$	$k(W/mK)$	σ (S/m)	β (K^{-1})
MoS_2	5060	397.21	904.4	2.09 x 10^4	2.8424 x 10^{-5}
Cu	8933	385	400	59.6 x 10^6	1.67 x 10^{-5}
$C_6H_2O_6$	1109	2400	0.258	5.5 x 10^{-6}	5.7 x 10^{-1}

Table 2. The related results of $-\theta'(0)$ incorporating $M = P = \gamma = \delta = \lambda = We = \phi_1 = \phi_2 = 0$, $\xi = \pi/2$, $B \to \infty$ and different values of Prandtl number [56-58] [created by author]

Pr	Ishak and Nazar [57]	Elbashbeshy et al. [58]	Paul et al. [56]	Current study
1	1	1	1.0005	1
10	3.7207	3.7207	3.72	3.7207

(MoS_2) with a solid volume percentage of 0.1 is integrated to the base fluid, ethylene glycol, followed by copper (Cu) nanoparticles with a solid volume concentration of 0.02. This volume ratio doesn't change while the issue is being investigated. As a base fluid, ethylene glycol is used. The thermo-physical features of the hybrid nanoparticle and the basic fluid are summarised in Table 1. The MATLAB Bvp4c method is used to evaluate the numerical results for the velocity and heat distribution. Compared to other studies, this one demonstrates a greater level of data accuracy. Table 2 lists many results for the rate of thermal transport in contrast to other studies showed by Ishak and Nazar [57], Elbashbeshy et al. [58], and Paul et al. [56]. It demonstrates that the Bvp4c approach is successful in producing computational results that are correct and reliable with the results of the other methods.

In Figure 2, how the heat stratification factor influenced the heat profile is displayed. The heat profile diminishes as heat stratification hikes. Substantial temperature variances between the layers caused by strong thermal stratification preserve the denser, colder fluid at the bottom of the fluid and the lighter, warmer fluid at the top. The fluid's inability to mix convectively due to this stratified structure stops thermal energy from being dispersed throughout the fluid volume. Also, the fluid surrounding the cylinder can be colder than the ambient whenever there is appropriate thermal stratification, generating the temperature to lessen. Deka and Paul [59] established that a greater stratification causes fluid flow to opposing across an infinite vertical cylinder. Besides, in our investigation, we have attained the same outcome for Cu/MoS_2 -$C_6H_2O_6$ Casson Williamson hybrid nanofluid movement.

Figure 3 illustrates that as the Weissenberg number (We) upsurges, the velocity profile declines, as advancing Weissenberg number growths viscosity, which upsurges resistance to fluid movement and shrinkages velocity. Figure 4 demonstrates how the Weissenberg number affects the heat profile. Temperature has a direct relationship with the Weissenberg number. Therefore, when the Weissenberg number increases, so does the thermal curve. Enhancing the Weissenberg number emphasizes greater stretching and alignment of fluid elements by exhibiting greater elastic

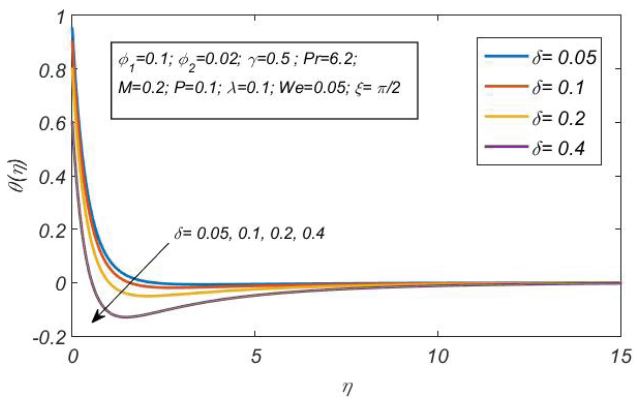

Figure 2. Illustration of temperature with stratification term.

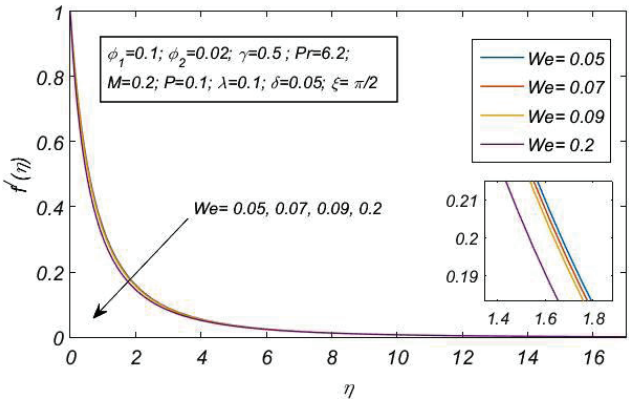

Figure 3. Illustration of velocity with Weissenberg number.

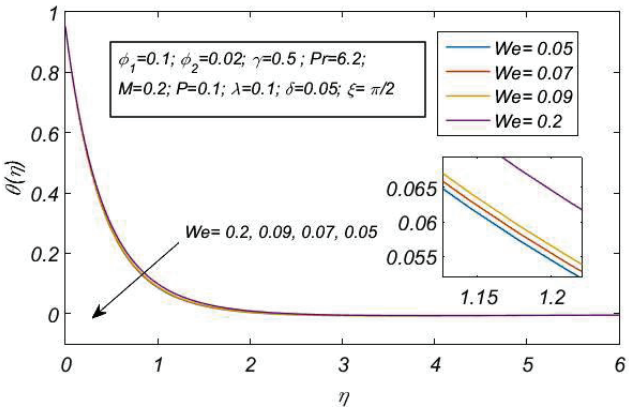

Figure 4. Influence on temperature with Weissenberg number.

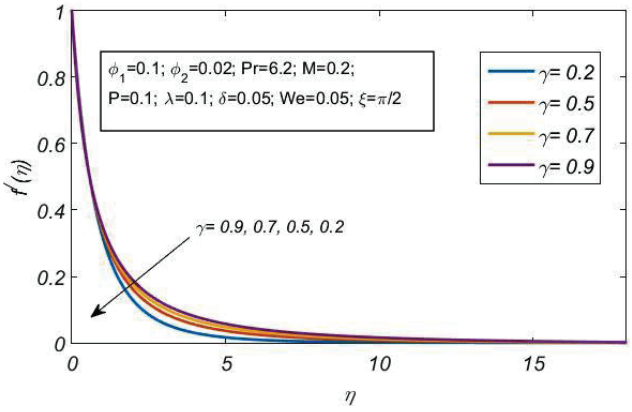

Figure 5. Illustration of velocity with curvature factor.

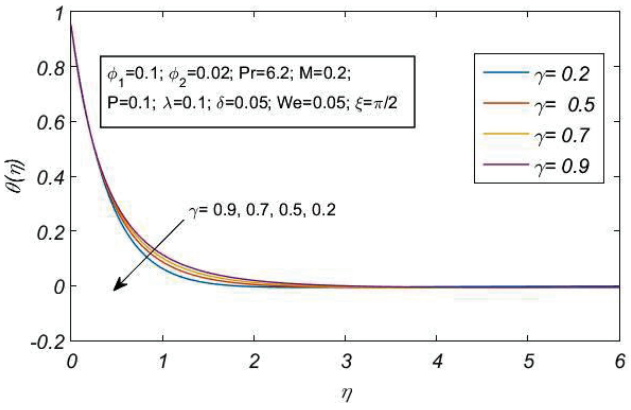

Figure 6. Illustration of temperature with curvature factor.

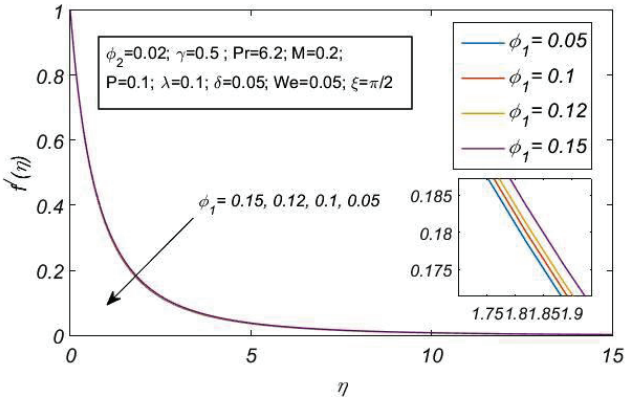

Figure 7. Demonstration of volume proportion (ϕ_1) of MoS_2 on velocity profile.

effects in non-Newtonian fluids. This optimizes heat transport inside the fluid and improves internal energy dissipation. Paul and Nath [32] obtained the same findings for both velocity and thermal curves without thermal stratification influence.

Figures 5 and 6 display how flow and the thermal profile are affected by the curvature factor γ. It appears that when γ broadens, fluid velocity increases. The circumference of the cylinder reduces as γ grows because the radius of curvature decreases. As a result, fluid particle impedance inside the cylinder decreases and fluid velocity increases. Additionally, the temperature curves increase as the size of γ increases. The thickness of the boundary layer increases with an increase in the curvature parameter, which improves thermal diffusion in the fluid. As a result of the enhanced heat flow throughout the layer, temperature curves are raised.

The influence of the volume fraction of MoS_2 on both the velocity and temperature gradient curves are exemplified in Figures 7 and 8, while the volume fraction of Cu remains constant. It is detected that both the flow velocity and heat distribution upsurge with advancement in the volume fraction of MoS_2 nanoliquids.

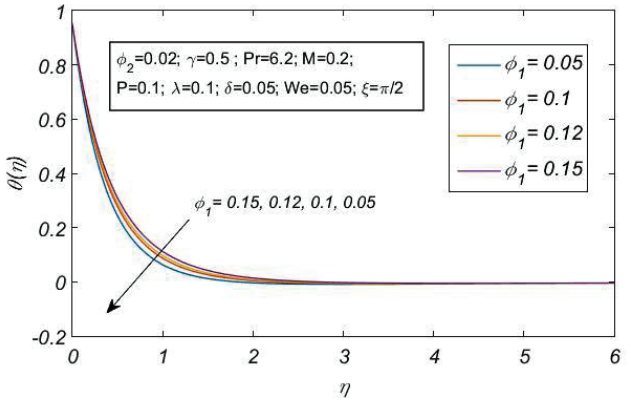

Figure 8. Demonstration of volume proportion (ϕ_1) of MoS_2 on heat distribution.

The skin friction coefficient and thermal transport rate are computed via the distinct noteworthy factors like the We, δ, and γ while ϕ_1= 0.1 and ϕ_2= 0.02 in Table 3. An enhancement in the skin friction, and the rate of heat

Table 3. Skin-friction and Nusselt number for changing value of *We, δ, γ* when ϕ_1= 0.1 and ϕ_2= 0.02

We	*δ*	*γ*	*Skin-Friction Coefficient*	*Nusselt Number*
0.05	0.01	0.1	2.4776	2.5218
0.08			2.4888	2.5186
0.1			2.5016	2.5122
0.3			2.7276	2.4768
0.05	0.03	0.1	2.4796	2.5198
	0.08		2.4845	2.5148
	0.2		2.4964	2.5029
	0.4		2.5163	2,4827
	0.6		2.5362	2.4624
0.05	0.01	0.1	2.4776	2.5218
		0.5	2.9948	2.7508
		0.7	3.2487	2.8622
		1.2	3.8707	3.1332

Table 4. Skin-friction and Nusselt number for varying magnitude of *B, P, λ* when ϕ_1= 0.1 and ϕ_2= 0.02

B	*P*	*γ*	*Skin-Friction Coefficient*	*Nusselt Number*
0.5	0.1	0.1	3.7819	2.7702
0.7			3.2840	2.7539
0.9			2.9984	2.7417
1.2			2.7412	2.7284
0.9	0.1	0.1	2.9984	2.7417
	0.4		3.2348	2.7216
	0.8		3.5265	2.6966
	1.2		3.7962	2.6734
0.9	0.1	0.1	2.9984	2.7417
		0.3	2.9557	2.7441
		0.5	2.9132	2.7464
		0.7	2.8708	2.7486

Table 5. Contrast of the Skin friction and Nusselt numbers for $Cu/C_6H_2O_6$ Casson Williamson-nanoliquid and $Cu\text{-}MoS_2$ / $C_6H_2O_6$ Casson Williamson-hybrid- nanoliquid

***Cu*/Ethylene Glycol**				***Cu-MoS*$_2$ /Ethylene Glycol**			
$\phi_1(MoS_2)$	$(\phi_2(Cu)$	**Skin Friction**	**Nusselt Number**	$\phi_1(MoS_2)$	$(\phi_2(Cu)$	**Skin Friction**	**Nusselt Number**
0	0.02	2.2925	2.3521	0.1	0.02	2.9984	2.7417
	0.03	2.3759	2.3924		0.03	3.0932	2.7907
	0.04	2.4606	2.4333		0.04	3.1899	2.8403
	0.05	2.5468	2.4747		0.05	3.2887	2.8905
	0.09	2.9083	2.6462		0.09	3.7067	3.0987

transference is reported with intensifying *γ*. Moreover, increasing magnitude of *We*, and *δ*, the rate of shear stress is also escalated.

The friction drag coefficient and Nusselt number are computationally simulated against numerous factors, such as the Casson factor, Porosity term, and Thermal buoyancy

parameter in Table 4. An enhancement in the absolute value of friction drag is noticed for boosting the Porosity factor (P), but the trend is the opposite for escalating the Casson (B) and Thermal buoyancy factor (γ). Moreover, the thermal transmission rate is improved for enlarging the heat buoyancy factor but decreases for boosting the value of the Casson and porosity factor.

Table 5 shows that enhancing the volume fraction of *Cu* nano-particles, keeping $\phi_1 = 0$ leads to advances in skin friction and the Nusselt number. Also, the heat transmits rate advances by more than 16.5% while the volume fraction of MoS_2 is 0.1. Moreover, it has been visible that the MoS_2 - *Cu*/ Ethylene glycol Casson Williamson hybrid nanofluid's absolute skin friction augmented by more than 30.7%.

CONCLUSION

The movement of MHD Casson Williamson Ethylene glycol based MoS_2 - *Cu* Hybrid nano-fluid via a linearly stretch vertical cylinder integrating the heat stratification impact and inclined magnetic field have been inspected numerically by employing the Bvp4c approach. The is also taken into consideration in this investigation. The impressions of governing factors on flow velocity and temperature distribution are demonstrated pictorially, along with their impacts on the Nusselt number and skin friction. The following are the main conclusions of this investigation:

- While there is adequate heat stratification, the temperature tends to be negative for ethylene glycol-based MoS_2 - *Cu* Casson Williamson hybrid nanoliquid.
- The rate of thermal transmission is decreasing for the augmenting thermal stratification, Casson and Williamson factors. Moreover, higher as the curvature and thermal buoyancy increase.
- The heat profile escalates with the augmented values of the Weissenberg number and curvature factor.
- Noteworthy expansion in the velocity profile is observed with the improving curvature term, but the opposite pattern is noticed for the Weissenberg number.
- The absolute value of friction drag is enhanced for rising Weissenberg number, thermal stratification, and curvature factor.
- The heat transfer speed goes up by more than 16.5% for MoS_2 - *Cu*/ Ethylene glycol Williamson hybrid nano-liquid in contrast with *Cu*/ Ethylene glycol Williamson nanoliquid.
- Casson Williamson hybrid nano-liquid has a thermal transport rate that is clearly advanced than that of Casson Williamson nanofluid.
- Enhancing the volume fraction of MoS_2 nanoparticle, while the volume fraction of *Cu* nanoparticle is constant, with both the velocity and thermal profile escalating.

Future directions for this research include investigating non-Newtonian fluid practices across multiple geometries, combining experimental validation with numerical simulations, and examining more intricate hybrid nanofluids with varied nanoparticle combinations for boosted thermal properties.

NOMENCLATURE

$(C_p)_f$	Specific heat capacity of fluid ($J\,kg^{-1}\,K^{-1}$)
$(C_p)_{hnf}$	Hybrid nanofluid's specific thermal capacity ($J\,kg^{-1}\,K^{-1}$)
$(C_p)_{s1}$	Specific thermal capacity of the MoS_2 ($J\,kg^{-1}\,K^{-1}$)
$(C_p)_{s2}$	Specific thermal capacity of the Cu ($J\,kg^{-1}\,K^{-1}$)
Gr_x	Grashof term
k_f	Heat conductivity of fluid ($Wm^{-1}\,K^{-1}$)
k_{bf}	Heat conductivity of nano-fluid ($Wm^{-1}\,K^{-1}$)
k_{hnf}	Heat conductivity of hybrid nano-fluid ($Wm^{-1}\,K^{-1}$)
k_{s1},k_{s2}	Heat conductivity of solid nanoparticles ($Wm^{-1}\,K^{-1}$)
k	Permeability (m^2)
M	Magnetic term
P	Porosity term
Pr	Prandtl Number
B	Casson factor
Re_x	Local Reynolds factor
T	Fluid temperature (K)
T_∞	Fluid's surroundings temperature (K)
T_w	Temperature at the wall (K)
w	The component of velocity in the r-direction(ms^{-1})
v	The component of velocity in the x direction (ms^{-1})
B_0	Strength of Magnetic field (NmA^{-1})
$(\beta_T)_f$	Fluid's thermal expansion (K^{-1})
$(\beta_T)_{s1}$	Thermal expansion of the MoS_2 (K^{-1})
$(\beta_T)_{s2}$	Thermal expansion Cu (K^{-1})
μ_f	Fluid's dynamic viscosity (mPa)
μ_{hnf}	Dynamic viscosity of hybrid nanofluid (mPa)
σ_{hnf}	Electric conductivity of the hybrid nanofluid ($Ohm^{-1}\,m^{-1}$)
ρ_f	Density of the fluid (kgm^{-3})
ρ_{hnf}	Density of the hybrid nanofluid (kgm^{-3})
ρ_{s1}	Density of MoS_2 (kgm^{-3})
ρ_{s2}	Density of Cu (kgm^{-3})
We	Weissenberg number
ϕ_1,ϕ_2	Volume fraction of MoS_2 and *Cu*
γ	The curvature parameter
δ	Thermal stratification factor
η	Similarity variable
λ	Heat buoyancy factor
ψ	Stream function

AUTHORSHIP CONTRIBUTIONS

Authors equally contributed to this work.

DATA AVAILABILITY STATEMENT

The authors confirm that the data that supports the findings of this study are available within the article. Raw data that support the finding of this study are available from the corresponding author, upon reasonable request.

CONFLICT OF INTEREST

The author declared no potential conflicts of interest with respect to the research, authorship, and/or publication of this article.

ETHICS

There are no ethical issues with the publication of this manuscript.

STATEMENT ON THE USE OF ARTIFICIAL INTELLIGENCE

Artificial intelligence was not used in the preparation of the article.

REFERENCES

[1] Kataria HR, Mittal AS. Mathematical model for velocity and temperature of gravity-driven convective optically thick nanofluid flow past an oscillating vertical plate in presence of magnetic field and radiation. J Niger Math Soc 2015;34:303–317. [CrossRef]

[2] Sheikholeslami M, Kataria HR, Mittal AS. Radiation effects on heat transfer of three dimensional nanofluid flow considering thermal interfacial resistance and micro mixing in suspensions. Chin J Phys 2017;55:2254–2272. [CrossRef]

[3] Kataria HR, Mittal AS. Velocity, mass and temperature analysis of gravity-driven convection nanofluid flow past an oscillating vertical plate in the presence of magnetic field in a porous medium. Appl Therm Eng 2017;110:864–874. [CrossRef]

[4] Sheikholeslami M, Kataria HR, Mittal AS. Effect of thermal diffusion and heat-generation on MHD nanofluid flow past an oscillating vertical plate through porous medium. J Mol Liq 2018;257:12–25. [CrossRef]

[5] Mittal AS, Kataria HR. Three dimensional CuO–Water nanofluid flow considering Brownian motion in presence of radiation. Karbala Int J Mod Sci 2018;4:275–286. [CrossRef]

[6] Akbarı N, Gholınıa M, Gholınıa S, Dabbaghıan S, Ganjı DD. Analytical and numerical study of hydrodynamic nano fluid flow in a two–dimensional semi-porous channel with transverse magnetic field. Sigma J Eng Nat Sci 2018;36:587–608.

[7] Li Z, Sheikholeslami M, Mittal AS, Shafee A, Haq RU. Nanofluid heat transfer in a porous duct in the presence of Lorentz forces using the lattice Boltzmann method. Eur Phys J Plus 2019;134:1–10. [CrossRef]

[8] Patel HR, Mittal AS, Darji RR. MHD flow of micropolar nanofluid over a stretching/shrinking sheet considering radiation. Int Commun Heat Mass Transf 2019;108:104322. [CrossRef]

[9] El Hattab M, Boumhaout M, Oukach S. MHD natural convection in a square enclosure using carbon nanotube-water nanofluid with two isothermal fins. Sigma J Eng Nat Sci 2024;42:1075–1087. [CrossRef]

[10] Maskeen MM, Zeeshan A, Mehmood OU, Hassan M. Heat transfer enhancement in hydromagnetic alumina–copper/water hybrid nanofluid flow over a stretching cylinder. J Therm Anal Calorim 2019;138:1127–1136. [CrossRef]

[11] Khashi'ie NS, Hafidzuddin EH, Arifin NM, Wahi N. Stagnation point flow of hybrid nanofluid over a permeable vertical stretching/shrinking cylinder with thermal stratification effect. CFD Lett 2020;12:80–94.

[12] Elsaid EM, Abdel-wahed MS. Impact of hybrid nanofluid coolant on the boundary layer behavior over a moving cylinder: Numerical case study. Case Stud Therm Eng 2021;25:100951. [CrossRef]

[13] Khan U, Zaib A, Ishak A, Sherif ESM, Waini I, Chu YM, et al. Radiative mixed convective flow induced by hybrid nanofluid over a porous vertical cylinder in a porous media with irregular heat sink/source. Case Stud Therm Eng 2022;30:101711. [CrossRef]

[14] Nath JM, Paul A, Das TK. Magnetohydrodynamics Stagnation Point Flow of Hybrid Nanofluids with Distinct Base Fluid over an Exponentially Extending Cylinder: A Numerical Comparative Analysis.Nano 2024;2450123. [CrossRef]

[15] Crane LJ. Boundary layer flow due to a stretching cylinder. Z Angew Math Phys 1975;26:619–622. [CrossRef]

[16] Wang CY. Fluid flow due to a stretching cylinder. Phys Fluids 1988;31:466–468. [CrossRef]

[17] Waqas H, Naqvi SMRS, Alqarni MS, Muhammad T. Thermal transport in magnetized flow of hybrid nanofluids over a vertical stretching cylinder. Case Stud Therm Eng 2021;27:101219. [CrossRef]

[18] Sreenivasa BR, Faqeeh JA, Alsaiari A, Alzahrani HA, Malik MY. Numerical study of heat transfer mechanism in the flow of ferromagnetic hybrid nanofluid over a stretching cylinder. Waves Random Complex Media 2022;1–17. [CrossRef]

[19] Nath JM, Das TK, Dey B. Flow of Newtonian and non-Newtonian hybrid nanofluid in cylindrical geometry. Nanofluids Technol Therm Sci Eng 2024;190–208. [CrossRef]

[20] Hamid A, Khan M, Khan U. Thermal radiation effects on Williamson fluid flow due to an expanding/contracting cylinder with nanomaterials: Dual solutions. Phys Lett A 2018;382:1982–1991. [CrossRef]

[21] Khan M, Salahuddin T, Malik MY, Mallawi FO. Change in viscosity of Williamson nanofluid flow due to thermal and solutal stratification. Int J Heat Mass Transf 2018;126:941–948. [CrossRef]

[22] Mittal AS, Patel HR, Darji RR. Mixed convection micropolar ferrofluid flow with viscous dissipation, joule heating and convective boundary conditions. Int Commun Heat Mass Transf 2019;108:104320. [CrossRef]

[23] Mittal AS, Patel HR. Influence of thermophoresis and Brownian motion on mixed convection two dimensional MHD Casson fluid flow with non-linear radiation and heat generation. Physica A: Stat Mech Appl 2020;537:122710. [CrossRef]
[24] Nath JM, Paul A, Das TK. Heat transfer characteristics of magnetohydrodynamic Casson stratified hybrid nanofluid flow past a porous stretching cylinder. J Thermal Eng 2021;10:1137–1148. [CrossRef]
[25] Hussain Z, Hayat T, Alsaedi A, Ullah I. On MHD convective flow of Williamson fluid with homogeneous-heterogeneous reactions: A comparative study of sheet and cylinder. Int Commun Heat Mass Transf 2021;120:105060. [CrossRef]
[26] Bilal M, Siddique I, Borawski A, Raza A, Nadeem M, Sallah M. Williamson magneto nanofluid flow over partially slip and convective cylinder with thermal radiation and variable conductivity. Sci Rep 2022;12:1–15. [CrossRef]
[27] Almaneea A. Numerical study on heat and mass transport enhancement in MHD Williamson fluid via hybrid nanoparticles. Alexandria Eng J 2022;61:8343–8354. [CrossRef]
[28] Kataria HR, Mistry M, Mittal A. Influence of non-linear radiation on MHD micropolar fluid flow with viscous dissipation. Heat Transf 2022;51:1449–1467. [CrossRef]
[29] Rashad AM, Nafe MA, Eisa DA. Heat variation on MHD Williamson hybrid nanofluid flow with convective boundary condition and Ohmic heating in a porous material. Sci Rep 2023;13:6071. [CrossRef]
[30] Das TK, Paul A, Nath JM. Endo/exothermic analysis of Casson and Maxwell quadra hybrid nanofluid flow configured by pollutant concentration with thermal and solute jump. J Taibah Univ Sci 2024;18:2382940. [CrossRef]
[31] Nabwey HA, EL-Hakiem AMA, Khan WA, Abdelrahman ZM, Rashad AM, Hawsah MA. Magnetic williamson hybrid nanofluid flow around an inclined stretching cylinder with joule heating in a porous medium. Chem Eng J Adv 2024;18:100604. [CrossRef]
[32] Paul A, Nath JM. Magneto-Hydrodynamic Stagnation Point Flow of Casson Williamson Hybrid Nanofluid Incorporating Viscous Dissipation and Suction/Injection Effect Past an Exponentially Stretching Cylinder. J Nanofluids 2024;13:710–720. [CrossRef]
[33] Das TK, Paul A, Nath JM. Thermo-convection driven Sodium Alginate-based Darcy–Forchheimer EMHD Williamson hybrid nanofluid flow with varying thermal distribution. Mod Phys Lett B 2024;2450405. [CrossRef]
[34] Srinivasacharya D, Surender O. Non-similar solution for natural convective boundary layer flow of a nanofluid past a vertical plate embedded in a doubly stratified porous medium. Int J Heat Mass Transf 2014;71:431–438. [CrossRef]
[35] Srinivasacharya D, Surender O. Non-darcy mixed convection induced by a vertical plate in a doubly stratified porous medium. J Porous Media 2014;17. [CrossRef]
[36] Srinivasacharya D, Surender O. Double Stratification effects on mixed convection along a vertical plate in a non-Darcy porous medium. Procedia Eng 2015;127:986–993. [CrossRef]
[37] Srinivasacharya D, Surender O. Effect of double stratification on mixed convection boundary layer flow of a nanofluid past a vertical plate in a porous medium. Appl Nanosci 2015;5:29–38. [CrossRef]
[38] Srinivasacharya D, Motsa SS, Surender O. Numerical study of free convection in a doubly stratified non-darcy porous medium using spectral quasi-linearization method. Int J Nonlinear Sci Numer Simul 2015;16:173–183. [CrossRef]
[39] Bilal S, Rehman KU, Malik MY. Numerical investigation of thermally stratified Williamson fluid flow over a cylindrical surface via Keller box method. Results Phys 2017;7:690–696. [CrossRef]
[40] Khan M, Salahuddin T, Malik MY, Mallawi FO. Change in viscosity of Williamson nanofluid flow due to thermal and solutal stratification. Int J Heat Mass Transf 2018;126:941–948. [CrossRef]
[41] Ramzan M, Gul N, Chung JD, Kadry S, Chu YM. Numerical treatment of radiative Nickel–Zinc ferrite-Ethylene glycol nanofluid flow past a curved surface with thermal stratification and slip conditions. Sci Rep 2020;10:1–14. [CrossRef]
[42] Khan MN, Ahmad S, Nadeem S. Flow and heat transfer investigation of bio–convective hybrid nanofluid with triple stratification effects. Phys Scr 2021;96:065210. [CrossRef]
[43] Masood S, Farooq M. Influence of thermal stratification and thermal radiation on graphene oxide-Ag/H2O hybrid nanofluid. J Therm Anal Calorim 2021;143:1361–1370. [CrossRef]
[44] Manzoor U, Muhammad T, Farooq U, Waqas H. Investigation of thermal stratification and nonlinear thermal radiation in Darcy-Forchheimer transport of hybrid nanofluid by rotating disk with Marangoni convection. Int J Ambient Energy 2022;1–8. [CrossRef]
[45] Kairi RR, Roy S, Raut S. Stratified thermosolutal Marangoni bioconvective flow of gyrotactic microorganisms in Williamson nanofluid. Eur J Mech B Fluids 2023;97:40–52. [CrossRef]
[46] Mohammadi H, Kumar S, Rezapour S, Etemad S. A theoretical study of the Caputo–Fabrizio fractional modeling for hearing loss due to Mumps virus with optimal control. Chaos Solitons Fract 2021;144:110668. [CrossRef]
[47] Khan H, Alzabut J, Shah A, He ZY, Etemad S, Rezapour S, et al. On fractal-fractional waterborne disease model: A study on theoretical and numerical aspects of solutions via simulations. Fractals 2023;31:2340055. [CrossRef]

[48] Chávez-Vázquez S, Lavín-Delgado JE, Gómez-Aguilar JF, Razo-Hernández JR, Etemad S, Rezapour S. Trajectory tracking of Stanford robot manipulator by fractional-order sliding mode control. Appl Math Modelling 2023;120:436–462. [CrossRef]

[49] Salahuddin T, Iqbal MA, Bano A, Awais M, Muhammad S. Cattaneo-Christov heat and mass transmission of dissipated Williamson fluid with double stratification. Alexandria Eng J 2023;80:553–558. [CrossRef]

[50] Farooq U, Waqas H, Makki R, Ali MR, Alhushaybari A, Muhammad T, Imran M. Computation of Cattaneo-Christov heat and mass flux model in Williamson nanofluid flow with bioconvection and thermal radiation through a vertical slender cylinder. Case Stud Therm Eng 2023;42:102736. [CrossRef]

[51] Alsallami SA, Abbas T, Al-Zubaidi A, Khan SU, Saleem S. Analytical assessment of heat transfer due to Williamson hybrid nanofluid (MoS2+ ZnO) with engine oil base material due to stretched sheet. Case Stud Therm Eng 2023;51:103593. [CrossRef]

[52] Salahuddin T, Fatima G, Awais M, Khan M, Al Awan B. Adaptation of nanofluids with magnetohydrodynamic Williamson fluid to enhance the thermal and solutal flow analysis with viscous dissipation: A numerical study. Results Eng 2024;21:101798. [CrossRef]

[53] Farooq U, Safeer M, Cui J, Hussain M, Naheed N. Forced convection analysis of Williamson-based magnetized hybrid nanofluid flow through a porous medium: Nonsimilar modeling. Numer Heat Transf B Fundam 2024;1–17. [CrossRef]

[54] You X, Wang Y. Series Solutions of Three-Dimensional Magnetohydrodynamic Hybrid Nanofluid Flow Heat Transf Nanomater 2024;14:316. [CrossRef]

[55] Shampine LF, Kierzenka J, Reichelt MW. Solving boundary value problems for ordinary differential equations in MATLAB with bvp4c. Tutorial Notes 2000;1–27.

[56] Paul A, Nath JM, Das TK. An investigation of the MHD Cu-Al2O3/H2O hybrid-nanofluid in a porous medium across a vertically stretching cylinder incorporating thermal stratification impact. J Therm Eng 2023;9:1300847. [CrossRef]

[57] Ishak A, Nazar R. Laminar boundary layer flow along a stretching cylinder. Eur J Sci Res 2009;36:22–29.

[58] Elbashbeshy EMA, Emam TG, El-Azab MS, Abdelgaber KM. Laminar boundary layer flow along a stretching cylinder embedded in a porous medium. Int J Phys Sci 2012;7:3067–3072. [CrossRef]

[59] Deka RK, Paul A. Transient free convection flow past an infinite moving vertical cylinder in a stably stratified fluid. Trans ASME J Heat Transfer 2012;134:0425031. [CrossRef]

[60] Unyong B, Vadivel R, Govindaraju M, Anbuvithya R, Gunasekaran N. Entropy analysis for ethylene glycol hybrid nanofluid flow with elastic deformation, radiation, non-uniform heat generation/absorption, and inclined Lorentz force effects. Case Stud Therm Eng 2022;30:101639. [CrossRef]

[61] Paul A, Nath JM, Das TK. Thermally stratified Cu–Al2O3/water hybrid nanofluid flow with the impact of an inclined magnetic field, viscous dissipation and heat source/sink across a vertically stretching cylinder. ZAMM J Appl Math Mech 2023;e202300084. [CrossRef]